

## Effect of UV Absorbers and Hindered Amine Light Stabilizers on the Photodegradation of Ethylene–Octene Copolymer

Zhongyang Liu, Shuangjun Chen, Jun Zhang

Department of Polymer Science and Engineering, College of Materials Science and Engineering, Nanjing University of Technology, Nanjing 210009, China

Correspondence to: J. Zhang (E-mail: zhangjun@njut.edu.cn)

**ABSTRACT:** The photodegradation behavior of ethylene–octene copolymer (EOC) and EOC stabilized with UV stabilizers (Tinuvin 326, Chimassorb 81, Tinuvin 770 and Chimassorb 944) were investigated by the digital photography, color difference, gel content, Fourier transform infrared spectroscopy (FTIR), differential scanning calorimetry (DSC), and mechanical tests. The results revealed that EOC exhibited a very poor photostability, whose performances were sharply reduced with increasing the irradiation time. The photodegradation products consisted of the carbonyl, hydroxyl and vinyl groups. The additives all showed an excellent photostabilizing effect, which effectively inhibited the gel formation and the chain photooxidation. The photostabilizing efficiency of these UV stabilizers could be ranked as Tinuvin 326 < Chimassorb 81 < Tinuvin 770 and Chimassorb 944. The secondary crystallization behavior was strongly affected by the annealing and chain scission. The chain scission, rather than the annealing, played a greater role in the secondary crystallization of the chain segments. And the serious chain scission could improve the mobility of the chain segments, which sharply promoted their crystallizability. © 2012 Wiley Periodicals, Inc. *J. Appl. Polym. Sci.* 000: 000–000, 2012

**KEYWORDS:** ethylene–octene copolymer; UV absorber; hindered amine light stabilizer; photodegradation; photostabilizing effect

Received 9 January 2012; accepted 20 April 2012; published online

DOI: 10.1002/app.37955

### INTRODUCTION

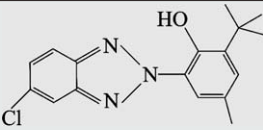
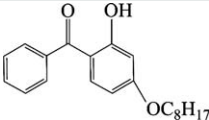

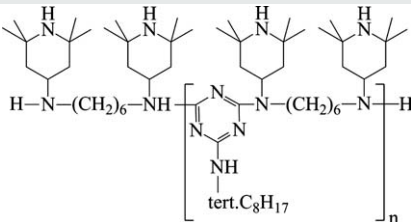
Ethylene–octene copolymer (EOC) produced by metallocene technology has good plasticity, high elongation, low rigidity, low density and excellent chemical stability.<sup>1–3</sup> It has fascinated more and more research attention in the industrial and academic fields, ascribed to the eminent properties. Bensason et al. classified EOC according to the comonomer content and studied the elasticity and deformation behavior.<sup>4–6</sup> Nicolás et al. investigated the properties of EOCs with high comonomer content crosslinked by dicumyl peroxide or  $\beta$ -radiation.<sup>7</sup> Experiments on the melting and crystallization behavior of EOC and the influence of deformation on the irreversible and reversible crystallization of EOC were carried out by Androsch et al.<sup>8–10</sup> The toughening applications of EOC as an impact modifier for the brittle polymers were widely reported.<sup>11–14</sup>

The polymeric materials exposed to the outdoor are typically subjected to sunlight, heat, humidity, atmospheric contaminants, oxygen and so forth. These factors could initiate the degradation of polymers, causing various irreversible chemical reactions and resulting in the deterioration of the useful characteristics.<sup>15,16</sup> Recently, more and more efforts have already

been devoted to studying the degradation behavior of EOC. Severini et al. reported the outdoor weathering of three different EOC films.<sup>17</sup> Hoàng et al. reported the thermooxidative degradation of EOC in the melting and solid state.<sup>18,19</sup> The effect of octene content, antioxidant and extrusion condition on the thermal degradation of EOC was reported by Al-Malaika et al.<sup>20–22</sup> Shang et al. investigated the biodegradation behavior of EOC/starch composites.<sup>23,24</sup> Bai et al. reported the photodegradation behavior of EOC and ethylene–hexene copolymer.<sup>25</sup> We investigated the influence of the octene concentration on the photodegradation behavior of EOC.<sup>26</sup> Even so, more attention still should be paid to the degradation behavior of EOC, especially for the photodegradation behavior of EOC. Controlling or restraining the photodegradation reactions of polymers used in the outside could effectively improve their service life. Generally, this could be accomplished by appropriately introducing a single additive or a combination of special additives (e.g. UV stabilizers and antioxidants) into the polymeric materials.<sup>27</sup> The chemical nature of the additives strongly influenced the long-time photostabilizing efficiency.<sup>28</sup> The published reports describing the effect of the additives on the photodegradation of polymers are voluminous. Bauer et al. investigated the

© 2012 Wiley Periodicals, Inc.

**Table I.** Structures and Characteristics of the Additives Used

Commercial name	Chemical structure	Physical properties
Tinuvin 326		Mw = 318.5 g/mol Tm = 138–141 °C
Chimassorb 81		Mw = 326.4 g/mol Tm = 48–49 °C
Tinuvin 770		Mw = 481 g/mol Tm = 81–85 °C
Chimassorb 944		Mw = 2000–3100 g/mol Tm = 100–135 °C

Mw, molecular weight; Tm, melting range.

influence of organic phosphites and hindered amine light stabilizers on the photooxidation of polypropylene.<sup>29</sup> The effect of the various combination of primary antioxidant, secondary antioxidant, UV absorber and hindered amine light stabilizer on the UV radiation stability and  $\gamma$ -radiation crosslinking of linear low density polyethylene and low density polyethylene was investigated by Basfar et al.<sup>30</sup> Jia et al. reported the combination effect of hindered amine light stabilizers and UV absorbers on the radiation resistance of polypropylene.<sup>31</sup> In our previous studies, the influence of UV absorbers, thermal stabilizers and the combination of UV absorbers and thermal stabilizers on the photostabilities of polyvinyl chloride was systematically investigated.<sup>32–36</sup> However, the photodegradation behavior of EOC added with UV absorber or hindered amine light stabilizer has not been reported yet.

Benzotriazole-type UV absorber, benzophenone-type UV absorber and hindered amine light stabilizer are extensively used for the stabilization of polymeric materials against UV light. As a following work, in this experiment, a benzotriazole-type UV absorber, a benzophenone-type UV absorber, a low molecular weight hindered amine light stabilizer and a high molecular weight hindered amine light stabilizer were used. Effect of these additives on the photodegradation behavior of EOC was investigated by digital photography, color difference, gel content, Fourier transform infrared (FTIR) spectroscopy, differential scanning calorimetry (DSC) and mechanical tests.

## EXPERIMENTAL

### Materials

EOC (Engage 8450) with a density of 0.902 g/cm<sup>3</sup> and a melt flow rate (190 °C/2.16 kg) of 3.0 g/10 min was supplied by the Dow Chemical Company, USA. Four types of UV stabilizers, a benzotriazole-type UV absorber [2-(2-hydroxy-3-tert-butyl-5-methylphenyl)-5-chlorobenzotriazole, Tinuvin 326], a benzophenone-type UV absorber [2-hydroxy-4-(octyloxy)benzophenone, Chimassorb 81], a low molecular weight hindered amine light stabilizer [bis-(2,2,6,6-tetramethyl-4-piperidinyl)sebacate, Tinuvin 770] and a high molecular weight hindered amine light stabilizer [poly[[6-[(1,1,3,3-tetramethylbutyl)amino]-1,3,5-triazine-2,4-diy]][(2,2,6,6-tetramethyl-4-piperidinyl)imino]-1,6-hexanediyl [(2,2,6,6-tetramethyl-4-piperidinyl)imino]], Chimassorb 944], used here were all purchased from Ciba Specialty Chemicals (China) Ltd., China. The structures and characteristics of these additives were shown in Table I.

### Sample Preparation and Artificial Accelerated Weathering

Table II listed the detailed formulation of different samples. The polymer resin and UV stabilizers were melt-blended in a torque rheogoniometer (XSS-300, Shanghai Kechuang Rubber Plastic Mechanical Equipment Co., Ltd., China) at 145 °C with a rotor speed of 80 rpm for 10 min. Then, the compound sheets of about 1.0 mm were prepared by hot-molding at 145 °C with a pressure of 10 MPa for 10 min. Finally, the dumbbell-shaped specimens were cut from the 1 mm sheets for the mechanical

**Table II.** Formulation of Samples Filled with Different Amount of UV Stabilizers

Sample name	Composition (phr)				
	EOC resin	Tinuvin 326	Chimassorb 81	Tinuvin 770	Chimassorb 944
EOC	100	-	-	-	-
U1	100	0.5	-	-	-
U2	100	-	0.5	-	-
H1	100	-	-	0.5	-
H2	100	-	-	-	0.5
U1H1	100	0.25	-	0.25	-
U1H2	100	0.25	-	-	0.25
U2H1	100	-	0.25	0.25	-
U2H2	100	-	0.25	-	0.25

Phr, parts by weight per hundred parts of resin.

tests, and the rectangular sheets were complemented for other analyses.

The artificial accelerated weathering was carried out in a xenon lamp test chamber (Q-SUN1000, Q-Panel Ltd., USA). According to ISO 4892-2, samples were irradiated at  $0.51 \text{ w/m}^2 @ \lambda = 340 \text{ nm}$  with the environmental temperature of  $65 \text{ }^\circ\text{C}$ . And the irradiation time ranged from 0 h to 1200 h.

#### Characterizations

Influence of the UV irradiation on the surfaces of samples was characterized by a stereomicroscope (Olympus SZ61, Olympus Company, Japan) and the photos were photographed using a color video camera (TK-C1481BEC, JVC, Japan).

Changes in the color difference between the unirradiated and irradiated samples were measured by a colorimeter (CR-300, Konica Minolta, Japan) according to ASTM D2244-89. The parameters ( $\Delta E$ ,  $\Delta L$ ,  $\Delta a$  and  $\Delta b$ ) were directly recorded by the colorimeter and they are associated by the following equation:

$$\Delta E = \sqrt{(\Delta L)^2 + (\Delta a)^2 + (\Delta b)^2} \quad (1)$$

where  $\Delta L$ ,  $\Delta a$  and  $\Delta b$  have the following meanings:  $+\Delta L$  = lighter,  $-\Delta L$  = darker;  $+\Delta a$  = redder,  $-\Delta a$  = greener;  $+\Delta b$  = yellower,  $-\Delta b$  = bluer.<sup>33,37</sup>

The exactly weighed samples were placed in a copper net with a mesh of 150. Then, they were extracted in a Soxhlet extractor for 48 h using xylene as an extractant. After extraction, samples were dried to a constant weight in a vacuum oven at  $80 \text{ }^\circ\text{C}$ . Finally, the residual weight of samples was weighted. The gel content was calculated using the following equation:<sup>38,39</sup>

$$\text{Gel content} = \frac{\text{Residual weight of sample}}{\text{Original weight of sample}} \times 100\% \quad (2)$$

The chemical structure changes were studied using a FTIR spectrometer (Nicolet iS5, Thermo Nicolet Corporation, USA) by the attenuated total reflection technique. Samples were analyzed at 32 scans in the region of  $4000 \text{ cm}^{-1}$  to  $650 \text{ cm}^{-1}$

with  $4 \text{ cm}^{-1}$  resolution. To eliminate the influence of the UV stabilizers on the FTIR spectra, the surfaces of samples before the FTIR measurements were scrubbed with alcohol until the obtained FTIR spectra were stable. The absorbance peak at  $2847 \text{ cm}^{-1}$  was selected as an internal reference to erase the thickness effect of samples. The photodegradation of the polymer matrix could generate carbonyl groups. Therefore, the carbonyl index (CI) was introduced here to quantify the photodegradation degree of samples, which was determined from the following relation:

$$CI = \frac{A_{1800-1650}}{A_{2847}} \quad (3)$$

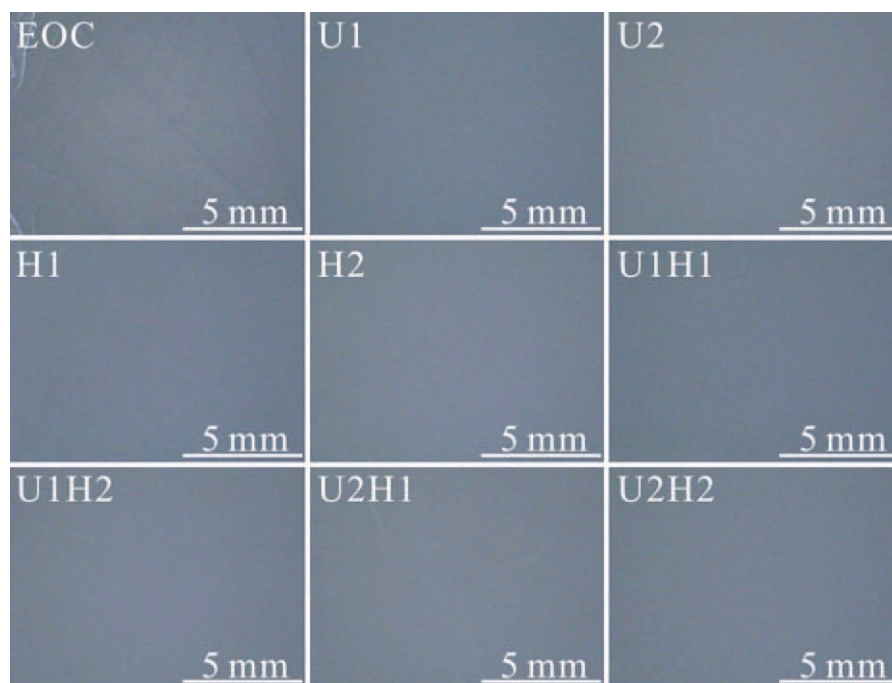
where  $A_{1800-1650}$  and  $A_{2847}$  are the integrated areas of the carbonyl groups ( $1800 \text{ cm}^{-1}$ – $1650 \text{ cm}^{-1}$ ) and the symmetrical stretching vibration of methylene ( $2847 \text{ cm}^{-1}$ ), respectively.

The DSC scans were performed on a differential scanning calorimeter (DSC Q200, TA instruments, USA) under nitrogen atmosphere with a flow rate of  $50 \text{ mL/min}$ . First, samples weighted about  $10 \text{ mg}$  were heated from  $-40 \text{ }^\circ\text{C}$  to  $140 \text{ }^\circ\text{C}$  with a heating rate of  $10 \text{ }^\circ\text{C/min}$ . Then, they were kept at  $140 \text{ }^\circ\text{C}$  for 3 min. Finally, they were cooled to  $-40 \text{ }^\circ\text{C}$  with a cooling rate of  $5 \text{ }^\circ\text{C/min}$ . The characteristic temperatures and melting enthalpy of samples were directly obtained from the DSC curves. The crystallinity ( $X_c$ ) was calculated according to the following equation:

$$X_c = \frac{\Delta H_f}{\Delta H_f^*} \times 100\% \quad (4)$$

where  $\Delta H_f$  is the measured melting enthalpy and  $\Delta H_f^*$  is the melting enthalpy of the perfect crystal of polyethylene, taken as  $277.1 \text{ J/g}$ .<sup>40</sup>

According to ISO 527-1:1993, the mechanical properties of the unirradiated and irradiated samples were measured by an electronic universal testing machine (CMT5254, Shenzhen Sans Test Machine Company Limited, China) with a crosshead speed of  $50 \text{ mm/min}$ . The results reported were the average values of three specimens.



**Figure 1.** Surface morphologies of samples irradiated for 1200 h. [Color figure can be viewed in the online issue, which is available at [wileyonlinelibrary.com](http://wileyonlinelibrary.com).]

## RESULTS AND DISCUSSION

### Effect of the Irradiation Time on the Surface Morphologies

All unirradiated samples exhibited a flat surface (their photos of the surface morphologies were not shown here). However, as the irradiation time increased, the surface morphologies changed gradually. Figure 1 displayed the surface photos of samples irradiated for 1200 h. Only the surface of sample EOC was fully covered with cracks, whereas other samples added with UV stabilizers displayed little change in the surface morphologies. The changes in the surface morphologies of samples were reported to be related with their photodegradation extent.<sup>23,33</sup> This phenomenon implied that the polymer matrix (sample EOC) suffered from the serious photodegradation and the UV stabilizers could effectively increase the photostabilities of samples with additives.

### Effect of the Irradiation Time on the Color Difference

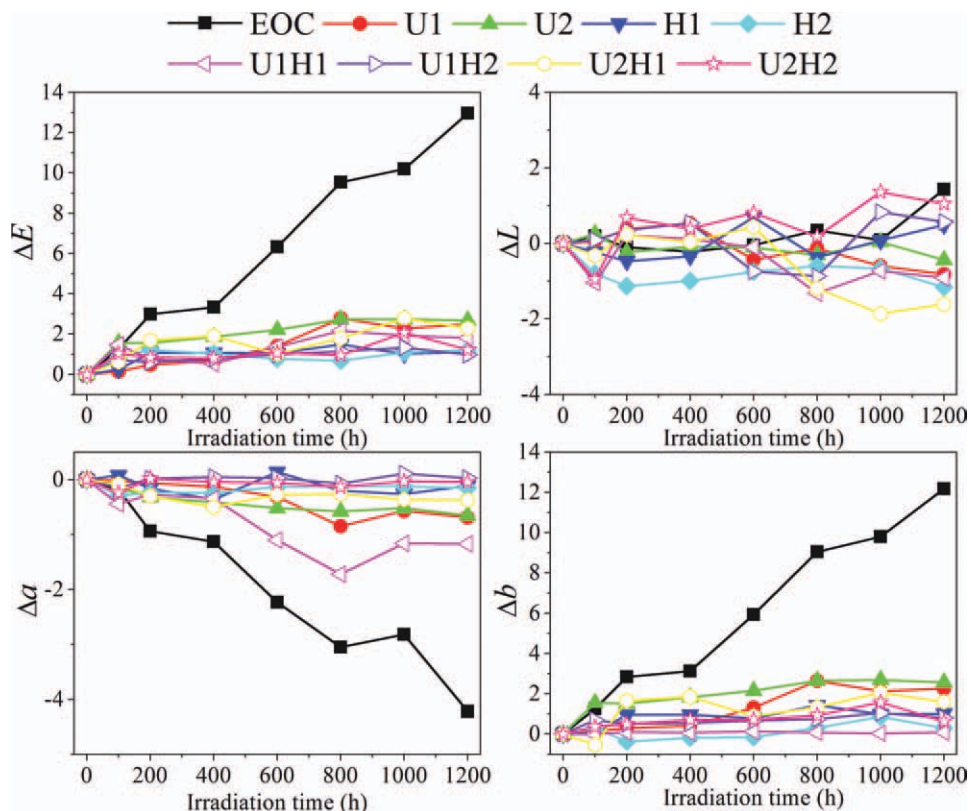
Figure 2 displayed the influence of the irradiation time on the color changes of different samples. The discoloration of samples was ascribed to the formation of the chromophore groups.<sup>41,42</sup> The color parameters ( $\Delta E$ ,  $\Delta a$  and  $\Delta b$ ) of sample EOC showed a significant change with increasing the irradiation time, whereas the  $\Delta L$  of sample EOC changed little. After irradiated for 200 h, the  $\Delta E$ ,  $\Delta a$  and  $\Delta b$  of sample EOC were 3.0,  $-0.9$  and 2.8, respectively. When the irradiation time reached 1200 h, they were increased to 13.0,  $-4.2$  and 12.2, respectively. It was shown that the  $\Delta b$  was the most important parameter to evaluate the discoloration of sample EOC. And the surface of sample EOC mainly shifted toward yellow.

It was well known that the appearances of Tinuvin 326 and Chimassorb 81 were slightly yellow powder, whereas those of

Tinuvin 770 and Chimassorb 944 were white granules and white to slightly yellowish granules, respectively. Compared with the unirradiated sample EOC, the color of some samples added with UV stabilizers changed because of the influence of the UV stabilizers. The color of the unirradiated samples added with Tinuvin 326 and Chimassorb 81 was turned to slightly yellow, whereas that of the unirradiated sample H1 and H2 changed a little. The color parameters ( $\Delta E$ ,  $\Delta L$ ,  $\Delta a$  and  $\Delta b$ ) of samples added with UV stabilizers were only vibrated in a small range, which may be partially attributed to the excellent photostabilizing effect of the UV stabilizers. It was worth noting that the color of the UV stabilizers also could conceal the discoloration of samples, which also resulted in the little change in the color difference of samples. That is to say, it was very possible that the yellow color of Tinuvin 326 and Chimassorb 81 covered the color changes of the corresponding samples.

### Effect of the Irradiation Time on the Gel Content

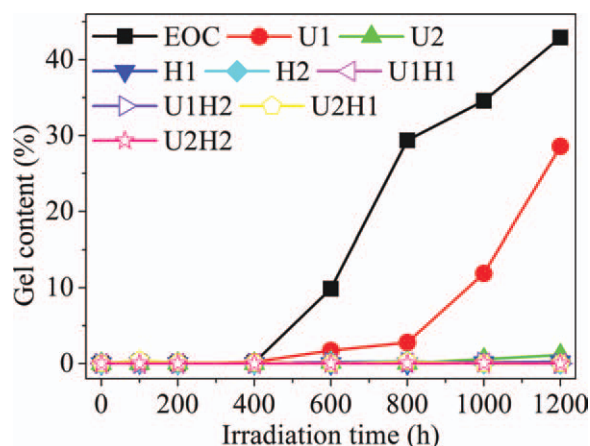
The photodegradation of polymers could produce radicals. Then, the reactions between the radicals generated the gel.<sup>43,44</sup> The gel content was usually used to evaluate the crosslinking extent of the polymer composites. Figure 3 revealed the gel content of samples before and after UV irradiation. During the first 400 h, the gel content of all samples was nearly zero. With the further increase in the irradiation time, the gel content of sample EOC was most significantly increased with the increase in the irradiation time. The gel content of sample EOC irradiated for 800 h and 1200 h reached 29% and 43%, respectively. In general, the gel content of the irradiated sample EOC was much bigger than that of other samples irradiated for the same time. It was reported that the UV stabilizers used here could inhibit the



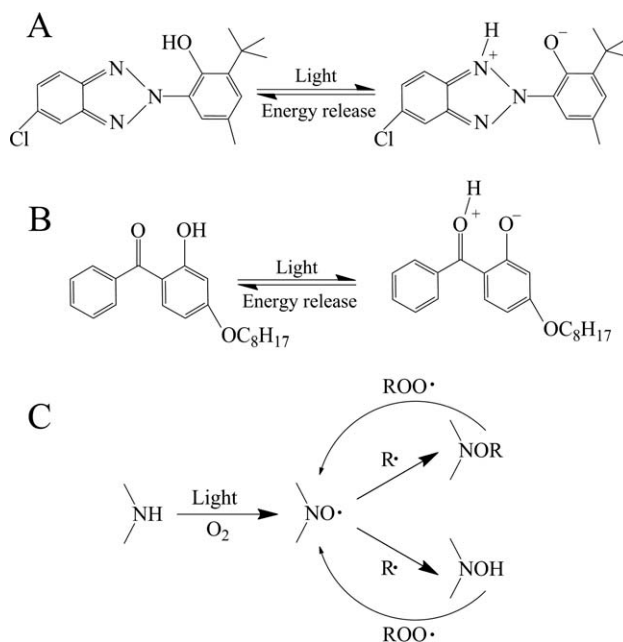
**Figure 2.** Effect of the irradiation time on the color difference of samples. [Color figure can be viewed in the online issue, which is available at [wileyonlinelibrary.com](http://wileyonlinelibrary.com).]

occurrence of the photodegradation reactions of polymers.<sup>27</sup> Correspondingly, the UV stabilizers, whose photostabilizing mechanisms were shown in Scheme 1,<sup>45–47</sup> were able to decrease the gel formation. The bigger the value of the gel content was, the more serious photodegradation the sample suffered from. The correlation between the gel content and the degradation degree of samples indicated that the photostability of EOC was very poor and the used additives had the photostabilizing

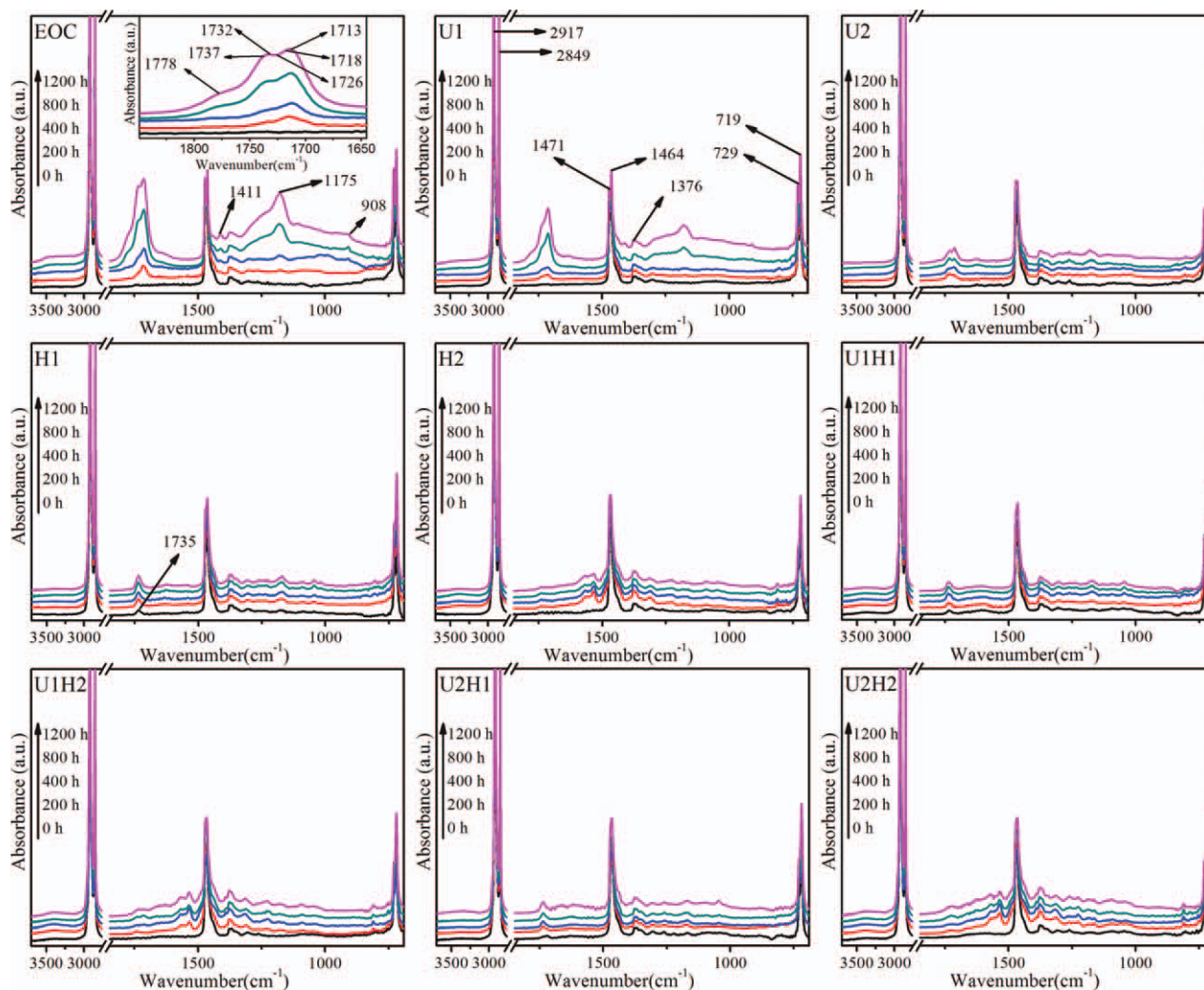
effect. As for samples with UV stabilizers, only sample U1 exhibited an obvious increasing trend in the gel content. During the irradiation period of 400 h–800 h, the gel content of sample



**Figure 3.** Effect of the irradiation time on the gel content of samples. [Color figure can be viewed in the online issue, which is available at [wileyonlinelibrary.com](http://wileyonlinelibrary.com).]



**Scheme 1.** Photostabilization mechanisms of (A) Tinuvin 326, (B) Chirmassorb 81, and (C) hindered amine light stabilizer.



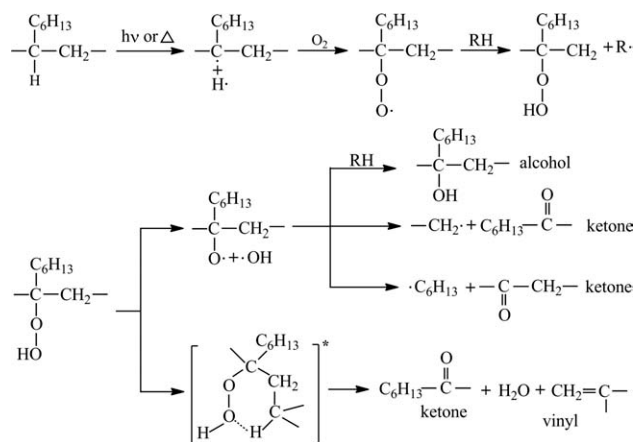
**Figure 4.** FTIR spectra of samples irradiated for various hours. [Color figure can be viewed in the online issue, which is available at [wileyonlinelibrary.com](http://wileyonlinelibrary.com).]

U1 was only slightly increased. After irradiated for 800 h, the gel content of sample U1 was 3%. Then, during the following irradiation time, the increasing degree of the gel content of the irradiated sample U1 was sharply increased. The gel content of sample U1 irradiated for 1200 h was up to 29%. As for sample U2, H1, H2, U1H1, U1H2, U2H1 and U2H2, their gel content changed little. Only the gel content of sample U2 irradiated for 1200 h was increased to 1.1%, whereas that of other samples irradiated for 1200 h was still not detected. These indicated that the efficiency of Tinuvin 326 on restraining the photocrosslinking was lower than that of other additives, especially during the irradiation period of 800 h–1200 h.

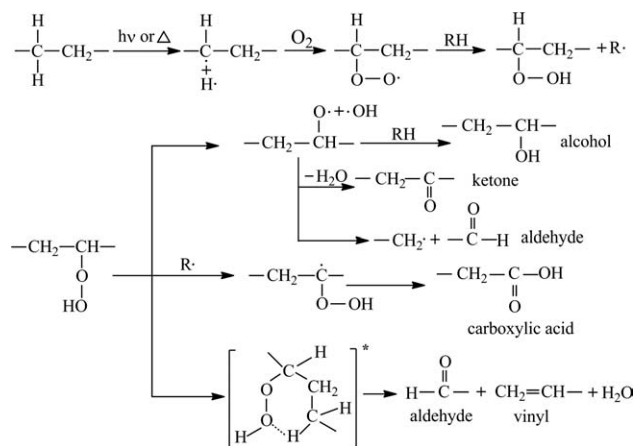
#### Effect of the Irradiation Time on the Chemical Structures

The FTIR spectra were used to analyze the chemical structure changes in the surfaces of different samples. Figure 4 showed the FTIR spectra of samples irradiated for 0 h, 200 h, 400 h, 800 h and 1200 h. As expected, most of the influence of the UV stabilizers on the FTIR spectra of samples could be eliminated through the pretreatment with alcohol. The spectra of all unirradiated samples displayed the characteristic absorbance peaks

of EOC. These typical peaks were as follows: 2917  $\text{cm}^{-1}$  and 2849  $\text{cm}^{-1}$  ascribed to the asymmetrical and symmetrical stretching vibration of  $-\text{CH}_2-$ ; 1471  $\text{cm}^{-1}$  attributed to the



**Scheme 2.** Photodegradation mechanism of the octene group.



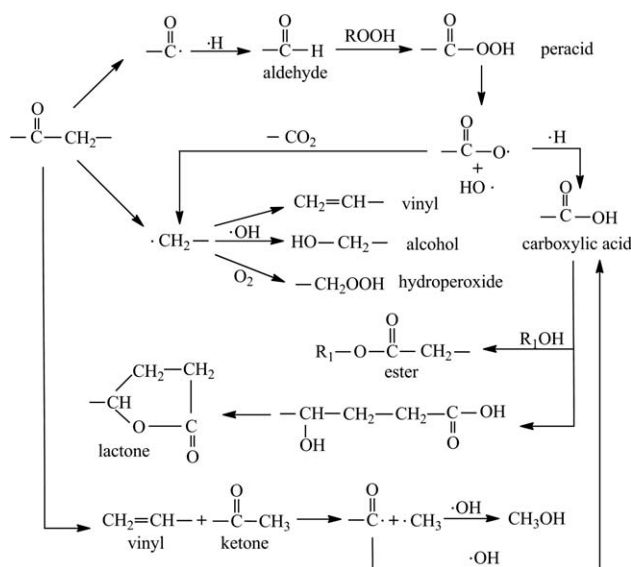
**Scheme 3.** Photodegradation mechanism of the ethylene group.

scissoring vibration of  $-\text{CH}_2-$ ;  $1464\text{ cm}^{-1}$  and  $1376\text{ cm}^{-1}$  assigned to the asymmetric and symmetrical bending vibration of  $-\text{CH}_3$ ;  $729\text{ cm}^{-1}$  and  $719\text{ cm}^{-1}$  attributed to the inner rocking vibration of  $-\text{CH}_2-$  in the crystalline and amorphous part.<sup>48–50</sup> In addition, a carbonyl absorption peak at  $1735\text{ cm}^{-1}$  was detected in the FTIR spectra of the unirradiated sample H1, U1H1 and U2H1, which should be ascribed to the ester carbonyl stretching vibration of Tinuvin 770.<sup>51</sup>

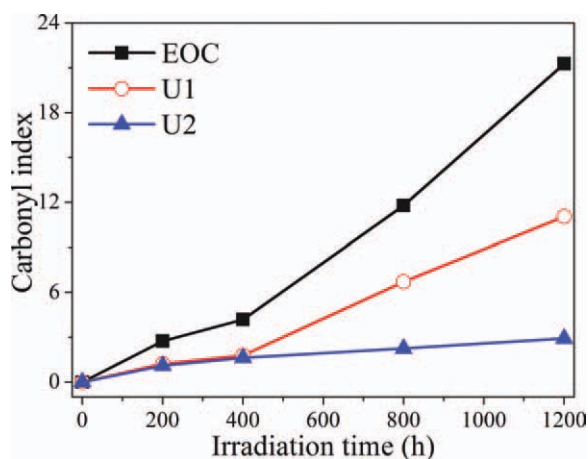
The hydrogens linked to tertiary carbons of the octene were very easily attacked by the UV light and oxygen. The formed peroxy radicals could yield the hydroperoxides by abstracting the labile hydrogen atoms and forming new free radical species.<sup>43,44</sup> And the hydroperoxide groups gave rise to a series of photodegradation reactions. The photodegradation mechanism of the octene was listed in Scheme 2.<sup>52</sup> Similarly, the ethylene groups could also be triggered by UV light, whose photodegradation mechanism was listed in Scheme 3.<sup>53</sup> The photodegradation degree was increased with increasing the irradiation time. The mechanisms of the photodegradation products were summarized in Scheme 4.<sup>44,54</sup> It was reported that the photodegradation products of EOC consisted of the dominant carbonyl groups as well as the hydroxyl and vinyl groups.<sup>26</sup> As observed in the FTIR spectra of sample EOC irradiated for various hours, new characteristic absorption peaks were emerged with increasing the irradiation time, whose intensity was also increased with the increase in the irradiation time. The absorbance region between  $3700\text{ cm}^{-1}$  and  $3100\text{ cm}^{-1}$  was attributed to the hydroxyl groups. In the carbonyl region, the absorbance at  $1778\text{ cm}^{-1}$  was due to the  $\text{C}=\text{O}$  stretching of lactone. The peak observed at  $1737\text{ cm}^{-1}$  was the ester carbonyl stretching vibration. The characteristic absorption band at  $1732\text{ cm}^{-1}$  corresponded to the carbonyl vibration of aldehyde. The presence of the chain-end ketone (methyl ketone) and the in-the-chain ketone (internal ketone) were proved by the peaks measured at  $1726\text{ cm}^{-1}$  and  $1718\text{ cm}^{-1}$ , respectively. The band at  $1713\text{ cm}^{-1}$  was ascribed to the  $\text{C}=\text{O}$  stretching of carboxylic acid. The peak at  $1175\text{ cm}^{-1}$  was due to the  $\text{C}-\text{O}$  stretching vibration of lactone.<sup>55,56</sup> It was considered that the absorbance at  $1411\text{ cm}^{-1}$  could be used to identify the internal ketone because it was related with the methylene deformation vibration in the long

chain ketone.<sup>57</sup> The chain-end unsaturation carbon-carbon double bond, attributed to the vinyl group, was detected by a peak at  $908\text{ cm}^{-1}$ .<sup>18</sup> It was found that the absorbance peaks of the hydroxyl and vinyl groups were very small even when the irradiation time was up to 1200 h. This was due to that these groups could easily change into other groups during the irradiation process.<sup>52</sup>

The different change degree in the FTIR spectra of different samples also revealed the different photostabilizing efficiency of different additives. Compared with sample EOC, only sample U1 showed the similar changes in the FTIR spectra, whereas the FTIR spectra of other samples exhibited the entirely different changes. The new generated groups of the irradiated sample U1 were nearly as the same as those of the irradiated sample EOC. However, the intensity of the characteristic absorption peaks of the photodegradation products of the irradiated sample U1 was much smaller than that of sample EOC irradiated for the same time. Compared with sample U1, the changes in the FTIR spectra of sample U2 were much smaller. Only the peaks in the carbonyl region were slightly increased with increasing the irradiation time. The FTIR spectra of sample H1, H2, U1H1, U1H2, U2H1 and U2H2 could be divided into two distinct types according to the change trends in their FTIR spectra. One type was composed of sample H1, U1H1 and U2H1, whose FTIR spectra changed little even when they were irradiated for 1200 h. The other one was made up of sample H2, U1H2 and U2H2. The FTIR spectra of the irradiated samples were obviously different from those of the unirradiated ones. However, there was no significant difference in the FTIR spectra among the different irradiated samples. And there were no obvious changes in the carbonyl region of the FTIR spectra of the irradiated sample H1, H2, U1H1, U1H2, U2H1 and U2H2. The intensity of the carbonyl region was very small. Considering that the formation of the carbonyl groups was taken as the main measurement criteria of the polymer photooxidation, the new formed absorption bands of the irradiated sample H1, H2, U1H1, U1H2,



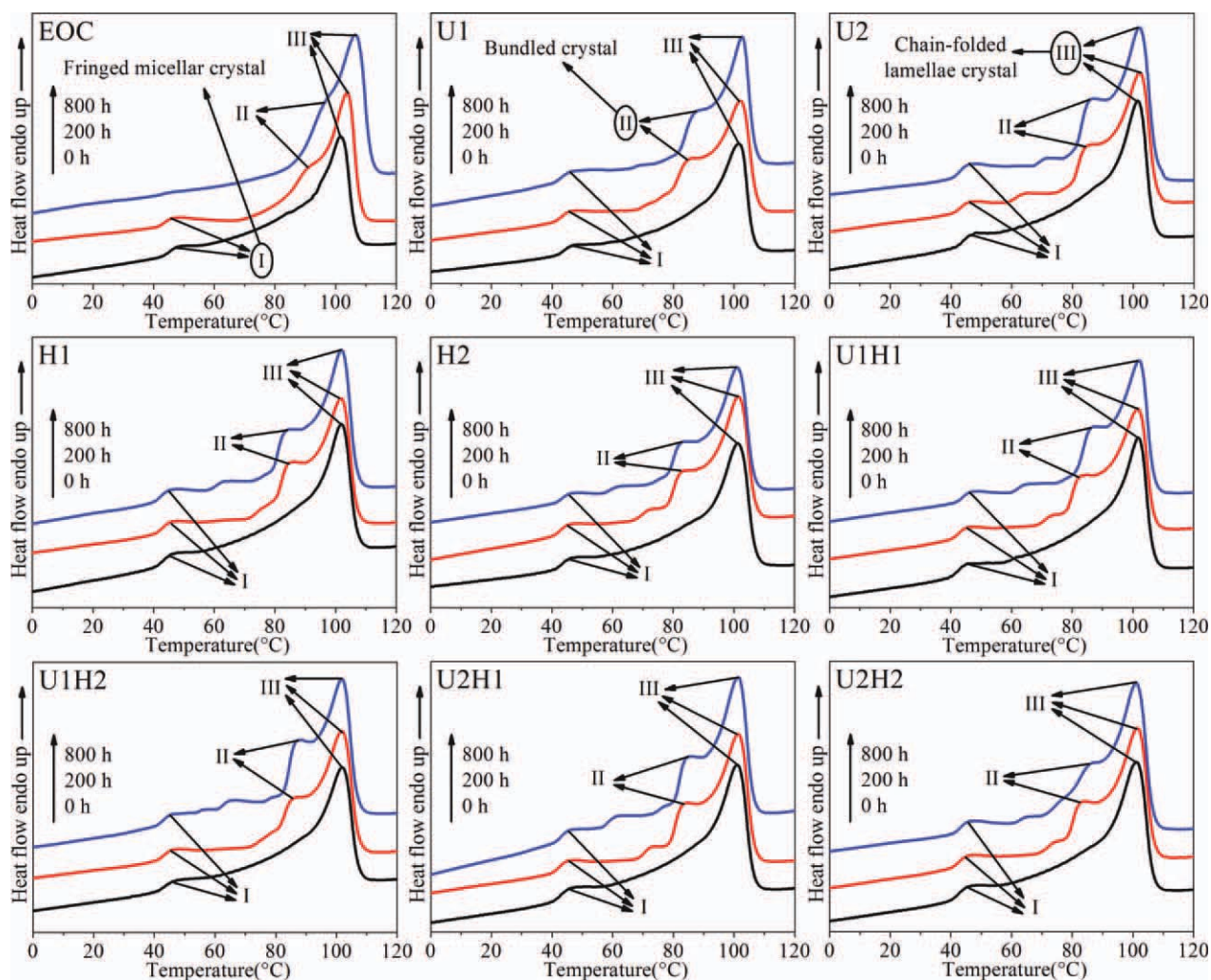
**Scheme 4.** Further degradation reactions of the oxidative products.



**Figure 5.** *CI* values of sample 1, 2, and 3 irradiated for various hours. [Color figure can be viewed in the online issue, which is available at [wileyonlinelibrary.com](http://wileyonlinelibrary.com).]

U2H1 and U2H2 should be ascribed to the results of the reactions between the UV stabilizers and the polymer matrix, instead of the photooxidative products of the polymer matrix. Therefore, calculating the *CI* values of sample H1, H2, U1H1, U1H2, U2H1 and U2H2 did not make any sense.

Figure 5 showed the *CI* values of sample EOC, U1 and U2 irradiated for various hours. The *CI* values of the unirradiated samples were about zero, which indicated that the effect of the sample preparation process on the sample degradation could be neglected. The *CI* values of all samples were increased with increasing the irradiation time. Sample EOC displayed the biggest increasing rate in the *CI* values. When irradiated for 800 h and 1200 h, the *CI* values of sample EOC reached 11.8 and 21.3, respectively. Relatively speaking, the increasing rate of the *CI* values of sample U1 and U2 was much lower. When irradiated for 1200 h, the *CI* values of sample U1 and U2 were only 11.1 and 2.9, respectively. The *CI* values were related with the photodegradation degree of samples. The higher the *CI* values



**Figure 6.** DSC melting curves of samples irradiated for 0 h, 200 h, and 800 h. [Color figure can be viewed in the online issue, which is available at [wileyonlinelibrary.com](http://wileyonlinelibrary.com).]



**Table III.** DSC Melting Parameters of Samples Irradiated for 0, 200, and 800 h

Sample	Aging time (h)	$T_I$ (°C)	$T_{II}$ (°C)	$T_{III}$ (°C)	$\Delta H_m$ (J/g)	$X_c$ (%)
EOC	0	47.6	-	101.6	92.2	33.3
	200	46.9	90.8	103.9	109.8	39.6
	800	-	95.7	106.5	118.5	42.8
U1	0	46.2	-	101.5	93.2	33.6
	200	45.9	84.7	102.1	100.9	36.4
	800	46.7	86.9	102.6	111.9	40.4
U2	0	46.1	-	101.5	91.9	33.2
	200	45.9	84.7	102.1	97.8	35.3
	800	45.2	86.2	102.0	103.9	37.5
H1	0	45.7	-	101.9	91.8	33.1
	200	45.8	84.4	101.7	96.7	34.9
	800	45.1	85.3	102.1	99.5	35.9
H2	0	46.2	-	101.2	92.7	33.5
	200	46.1	85.2	101.6	95.3	34.4
	800	45.5	84.7	101.1	98.4	35.5
U1H1	0	45.3	-	101.8	91.4	33.0
	200	45.5	84.5	101.4	95.6	34.5
	800	46.2	85.5	101.7	98.4	35.5
U1H2	0	46.1	-	101.8	91.6	33.1
	200	45.8	86.1	101.6	96.2	34.7
	800	47.8	87.9	101.4	97.8	35.3
U2H1	0	45.7	-	101.1	92.6	33.4
	200	45.3	84.8	101.5	96.7	34.9
	800	45.6	84.2	101.2	98.7	35.6
U2H2	0	45.4	-	101.1	92.5	33.4
	200	45.2	83.8	101.4	97.6	35.2
	800	45.9	85.7	101.1	98.9	35.7

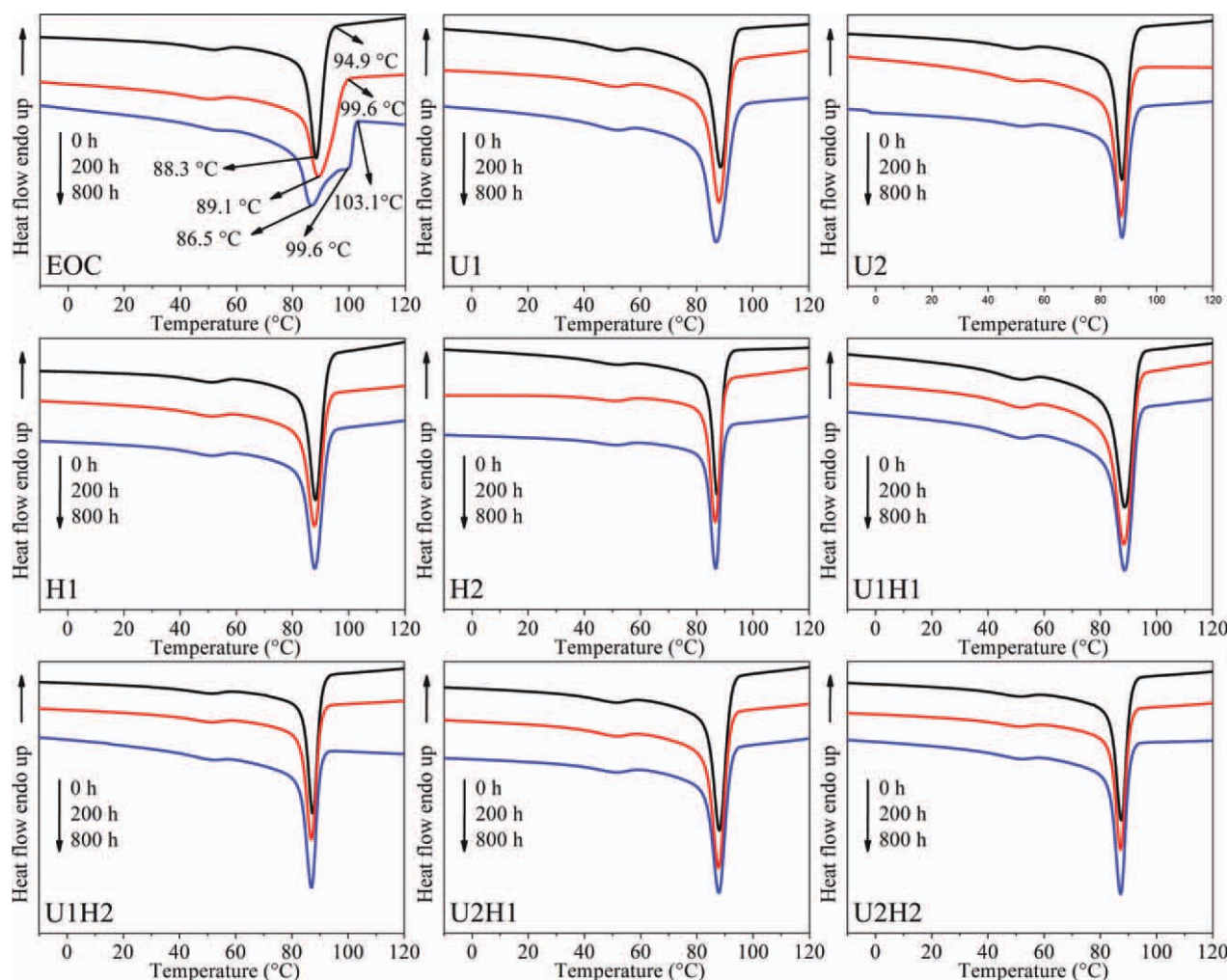
were, the more serious photodegradation samples suffered from. These again confirmed that sample EOC suffered from the most serious degradation and the photostabilizing efficiency of Chimassorb 81, Tinuvin 770 and Chimassorb 944 were much stronger than that of Tinuvin 326. It should be mentioned that the order of the photostabilizing efficiency of Tinuvin 326 and Chimassorb 81 on the photodegradation of EOC was contrary to that on the photodegradation of polyvinyl chloride.<sup>35,36</sup> EOC was a nonpolar polymer, whereas polyvinyl chloride was a polar polymer. There were more unstable structures in polyvinyl chloride than in EOC. These differences could influence the migration of the UV stabilizers and might affect the photostabilizing efficiency of the additives.

#### Effect of the Irradiation Time on the Melting and Crystallization Behavior

The DSC melting curves of samples irradiated for 0 h, 200 h, and 800 h were displayed in Figure 6 and the corresponding parameters were listed in Table III. In general, there was no obvious difference between the melting curves of all different unirradiated samples and two obvious melting peaks in the DSC melting curves of all unirradiated samples were observed. For example, the temperatures of the low melting peak (peak I) and the high one (peak III) of sample EOC were 47.6 °C and

101.6 °C, respectively. The melting peaks of other samples were also detected in the vicinity of the temperature regions of those of sample EOC. The  $\Delta H_m$  and  $X_c$  of all unirradiated samples displayed slight differences. These indicated that all samples experienced the similar thermal history during the sample preparation process and the UV stabilizers had little influence on the crystallization behavior of samples during the sample preparation process. The low melting peak was ascribed to the melting of the fringed micellar crystal, which was the product of the secondary crystallization of the most defective chain segments at the room temperature. Secondary crystallization was the common name for the crystallization process, which was exclusive of the crystallization process that samples were cooled to the room temperature during the sample preparation. The peak III was attributed to the melting of the chain-folded lamellae, generated by the long ethylene sequences.<sup>4,26</sup>

It was observed that the UV irradiation had an influence on the changes in the DSC melting curves of sample EOC. When irradiated for 200 h, the melting peak temperature of peak I ( $T_I$ ) and peak III ( $T_{III}$ ) of sample EOC changed a little, whereas the  $\Delta H_m$  and  $X_c$  were sharply increased, reaching 109.8 J/g and 39.6%, respectively. A new melting peak emerged in the melting curve, which was due to the melting of the bundled crystal,

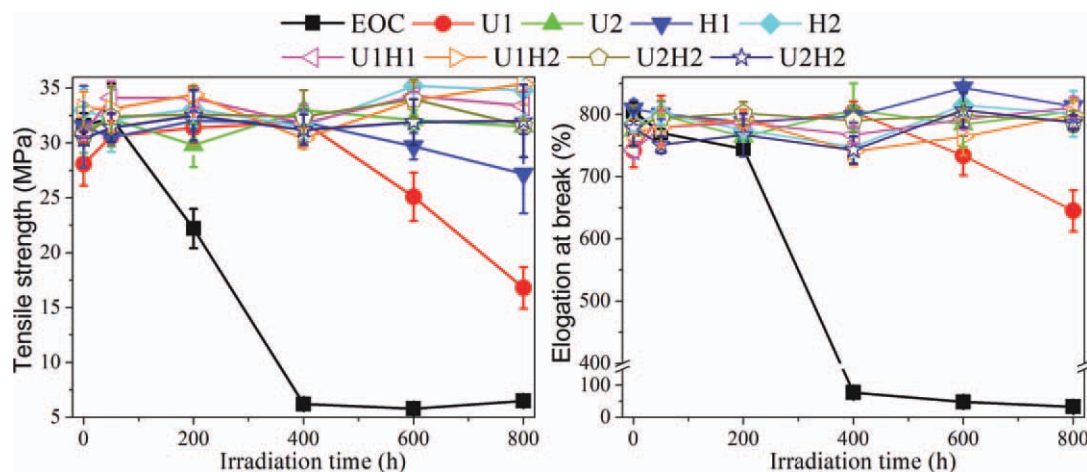


**Figure 7.** DSC crystallization curves of samples irradiated for 0 h, 200 h, and 800 h. [Color figure can be viewed in the online issue, which is available at [wileyonlinelibrary.com](http://wileyonlinelibrary.com).]

formed by the originally presented short ethylene sequences. For convenience, the melting peak of the bundled crystal, lower than peak III, was named as peak II. It should be mentioned that during the process of the sample preparation, most of the short ethylene sequences were not incorporated into the crystal lattice, ascribed to the lack of the effective mobility. When samples were irradiated at 65 °C, the annealing could promote secondary crystallization of the ethylene sequences. These induced that the melting peak of the bundled crystal appeared and the DSC parameters changed. With the further increase in the irradiation time, the  $T_I$  nearly disappeared, whereas the melting peak temperature of peak II ( $T_{II}$ ) and  $T_{III}$ ,  $\Delta H_m$  and  $X_c$  were further increased, up to 95.7 °C, 106.5 °C, 118.5 J/g and 42.8%, respectively. The disappearance of peak I of sample EOC irradiated for 800 h was attributed to that the serious photodegradation of the most defective chain segments at 65 °C rapidly decreased the amount of the most defective chain segments. It was believed that the melting temperature of the crystal was related with its size. Generally speaking, the bigger the crystal size was, the higher the melting temperature was.<sup>58,59</sup> Hence, the further increase in  $T_{II}$ ,  $T_{III}$ ,  $\Delta H_m$  and  $X_c$  was ascribed to

that the chain scission improved the mobility of the chain segments to form the bigger crystal.

Compared with sample EOC, the similar changes, such as the appearance of the melting peak of the bundled crystal, the increase in the  $\Delta H_m$  and  $X_c$  were also measured in the other eight samples irradiated for 200 h and 800 h. UV stabilizers decreased the photodegradation degree of the corresponding samples, which could influence the secondary crystallization behavior of the chain segments. These resulted in the difference in the melting behavior between the irradiated sample EOC and the irradiated samples with UV stabilizers. First, after irradiated for 800 h, the melting peak of the fringed micellar crystal was still observed in the melting curves of samples with UV stabilizers, which could be ascribed to that UV stabilizers had a stabilizing effect on the photodegradation of the chain segments. Second, the melting peak temperature of the bundled crystal of samples added with the UV stabilizers was much lower than that of sample EOC. Third, the increasing degree of the  $T_{II}$ ,  $T_{III}$ ,  $\Delta H_m$  and  $X_c$  was also much lower than that of sample EOC. The photostabilizing effect of the UV stabilizers restrained the



**Figure 8.** Tensile strength and elongation at break of samples irradiated for various hours. [Color figure can be viewed in the online issue, which is available at [wileyonlinelibrary.com](http://wileyonlinelibrary.com).]

chain scission, which slowed the increasing degree of the mobility and crystallizability of the chain segments. The chain scission, rather than the annealing, played a greater role in improving the mobility and crystallizability of the chain segments. Consequently, the increase in the  $\Delta H_m$  and  $X_c$  of sample EOC irradiated for 200 h was not only attributed to the annealing effect but also attributed to the chain scission.

There was only a little difference in the DSC melting curves of the irradiated samples with additives, which was due to that the different UV stabilizers with the different photostabilizing efficiency had a slightly different effect on the secondary crystallization of the chain segments. Among eight samples added with the UV stabilizers, sample U1 displayed the biggest increasing extent in the  $\Delta H_m$  and  $X_c$ , and sample U2 occupied the second position. The increasing degree in the  $\Delta H_m$  and  $X_c$  was linked to the degradation degree of samples. The bigger the increasing degree was, the more serious photodegradation samples suffered from.<sup>26,60</sup> These implied that the photostabilizing efficiency of Tinuvin 326 was lowest among the used UV stabilizers and the photostabilizing efficiency of Chimassorb 81 was lower than that of Tinuvin 770 and Chimassorb 944.

The following DSC crystallization curves of samples irradiated for 0 h, 200 h, and 800 h were presented in Figure 7. All unirradiated samples exhibited two crystallization peaks. The one at about 88 °C was the crystallization peak of the long ethylene sequences and the other one was about 51 °C, which was due to the crystallization peak of the short ethylene sequences. The little difference between the DSC crystallization curves of samples irradiated for 0 h showed that the UV stabilizers showed little nucleating effect on the crystallization behavior of polymer matrix and the changes in the crystallization curves of samples were only determined by the changes in the chain segments. The crystallization behavior of sample EOC significantly changed with the increase in the irradiation time. The photodegradation of the polymer matrix gave rise to not only the chain crosslinking but also the chain scission. And the fractured chains had a better mobility and crystallizability than the original chains. Hence, after irradiated for 200 h, the onset crystalli-

zation temperature was shifted to the higher region and the main crystallization peak was increased from 88.3 °C to 89.1 °C. When the irradiation time was up to 800 h, the main crystallization region widened significantly, due to the sharply increasing amount of the fractured chains. One of the crystallization peaks reached 99.6 °C, and the onset crystallization temperature was further augmented. These indicated that sample EOC suffered from the serious photodegradation when the irradiation time was up to 800 h and the serious chain scission could improve the mobility of the chain segments, which promoted their crystallizability. Attributed to the strong photostabilizing effect of the UV stabilizers, the chain segments of the irradiated samples with additives changed much less than that of the irradiated sample EOC. In addition, the crystallization behavior of samples in this study was only determined by the polymer chain segments. These led to the little difference in the crystallization curves between the unirradiated and irradiated sample U1, U2, H1, H2, U1H1, U1H2, U2H1 and U2H2. The crystallization curves of samples with UV stabilizers were similar to each other.

#### Effect of the Irradiation Time on the Mechanical Properties

Figure 8 showed the effect of the irradiation time on the tensile strength and elongation at break of samples. It was measured that the tensile strength and elongation at break of the unirradiated sample EOC were 31.6 MPa and 805%, respectively. When irradiated for 50 h, the tensile strength and elongation at break of sample EOC changed little. However, with increasing the irradiation time, the tensile strength and elongation at break of sample EOC were sharply decreased. When irradiated for 400 h, the tensile strength and elongation at break were decreased to 6.2 MPa and 77%, respectively. Then, the tensile strength and elongation at break changed little with the further increase in the irradiation time.

The small amount of UV stabilizers had no reinforcing effect on the mechanical properties of the unirradiated samples added with additives. Therefore, there was no obvious difference in the tensile strength and elongation at break between the unirradiated sample EOC and other unirradiated samples added with UV stabilizers. Among samples added with the UV stabilizers,

only sample U1 displayed a decrease trend in the tensile strength and elongation at break with increasing the irradiation time, whereas the tensile strength and elongation at break of other seven samples only fluctuated in a narrow range. When sample U1 was irradiated for 400 h, the tensile strength and elongation at break changed little, up to 31.9 MPa and 804%, respectively. When the irradiation time was up to 600 h, they were decreased to 25.1 MPa and 734%. With the further increase in the irradiation time, they reached 16.8 MPa and 645%, respectively. It seemed that the tensile strength of sample U1 was easier to be decreased by the UV irradiation than the elongation at break. The decrease in the mechanical properties of the irradiated sample U1 indicated that the photostabilizing efficiency of Tinuvin 326 was poorer than other UV stabilizers.

## CONCLUSIONS

This study revealed the influence of UV absorbers (Tinuvin 326 and Chimassorb 81) and hindered amine light stabilizers (Tinuvin 770 and Chimassorb 944) on the photodegradation behavior of EOC through a series of characterization methods. The performance losses of samples were qualitatively correlated with their degradation degree. The photodegradation reactions of the polymer matrix were very easily initiated by the UV light and the mechanical properties were significantly decreased with the increase in the irradiation time. The photodegradation products were made up of the predominant carbonyl groups as well as the hydroxyl and vinyl groups. All UV stabilizers displayed an excellent photostabilizing effect, which effectively restrained the formation of gel and the photodegradation of the chain segments. The photostabilizing efficiency of these additives could be ordered as follows: Tinuvin 326 < Chimassorb 81 < Tinuvin 770 and Chimassorb 944. The annealing and chain scission could strongly influence the secondary crystallization behavior of the crystallizable chain segments. The chain scission played a greater role than the annealing in the secondary crystallization of the chain segments. The serious chain scission could significantly improve the crystallizability of the polymer chains, attributed to the increasing mobility of the broken chains.

## ACKNOWLEDGMENTS

The financial support for this work was provided by the Priority Academic Program Development of Jiangsu Higher Education Institutions.

## REFERENCES

- Yuan, B.; Chen, X.; He, B. B. *J. Vinyl Addit. Technol.* **2008**, *14*, 45.
- Luo, W. A.; Yi, G. B.; Yang, J.; Liao, Z. F.; Chen, X. D.; Mai, K. C.; Zhang, M. Q. *J. Appl. Polym. Sci.* **2010**, *115*, 1015.
- Ray, S.; Bhowmick, A. K.; Swayajith, S. *J. Appl. Polym. Sci.* **2003**, *90*, 2453.
- Bensason, S.; Minick, J.; Moet, A.; Chum, S.; Hiltner, A.; Baer, E. *J. Polym. Sci. Part B: Polym. Phys.* **1996**, *34*, 1301.
- Bensason, S.; Nazarenko, S.; Chum, S.; Hiltner, A.; Baer, E. *Polymer* **1997**, *38*, 3913.
- Bensason, S.; Stepanov, E. V.; Chum, S.; Hiltner, A.; Baer, E. *Macromolecules* **1997**, *30*, 2436.
- Nicolás, J.; Ressia, J. A.; Vallés, E. M.; Merino, J. C.; Pastor, J. M. *J. Appl. Polym. Sci.* **2009**, *112*, 2691.
- Androsch, R. *Polymer* **1999**, *40*, 2805.
- Androsch, R.; Wunderlich, B. *Macromolecules* **2000**, *33*, 9076.
- Androsch, R.; Wunderlich, B.; Lüpke, T.; Wutzler, A. *J. Polym. Sci. Part B: Polym. Phys.* **2002**, *40*, 1223.
- Lee, H. Y.; Kim, D. H.; Son, Y. *J. Appl. Polym. Sci.* **2007**, *103*, 1133.
- Yan, X. L.; Xu, X. H.; Zhu, L. *J. Mater. Sci.* **2007**, *42*, 8645.
- Adhikari, R.; Godehardt, R.; Lebek, W.; Frangov, S.; Michler, G. H.; Radusch, H.; Calleja, F. J. B. *Polym. Adv. Technol.* **2005**, *16*, 156.
- Adhikari, R.; Godehardt, R.; Lebek, W.; Michler, G. H. *J. Appl. Polym. Sci.* **2007**, *103*, 1887.
- Amin, A.-R. *J. Polym. Environ.* **2001**, *9*, 25.
- Chen, S.; Zhang, J.; Su, J. *J. Appl. Polym. Sci.* **2009**, *114*, 3110.
- Severini, F.; Gallo, R.; Ipsale, S.; Nisoli, E.; Pardi, M. *Polym. Degrad. Stab.* **1999**, *65*, 329.
- Hoàng, E. M.; Allen, N. S.; Liauw, C. M.; Fontán, E.; Lafuente, P. *Polym. Degrad. Stab.* **2006**, *91*, 1356.
- Hoàng, E. M.; Allen, N. S.; Liauw, C. M.; Fontán, E.; Lafuente, P. *Polym. Degrad. Stab.* **2006**, *91*, 1363.
- Al-Malaika, S.; Peng, X.; Watson, H. *Polym. Degrad. Stab.* **2006**, *91*, 3131.
- Al-Malaika, S.; Peng, X. *Polym. Degrad. Stab.* **2007**, *92*, 2136.
- Al-Malaika, S.; Peng, X. *Polym. Degrad. Stab.* **2008**, *93*, 1619.
- Shang, X. Y.; Fu, X.; Yang, L. S.; Chen, X. D. *J. Reinf. Plast. Comp.* **2009**, *28*, 279.
- Shang, X. Y.; Fu, X.; Chen, X. D.; Yang, L. S. *J. Appl. Polym. Sci.* **2009**, *114*, 3574.
- Bai, F. C.; Zhang, C. X.; Zhang, X. Y.; Liu, J.; Tian, W. *Mater. Sci. Forum* **2009**, *610*, 243.
- Liu, Z.; Chen, S.; Zhang, J. *Polym. Degrad. Stab.* **2011**, *96*, 1961.
- Hussain, I.; Redhwi, H. *J. Mater. Eng. Perform.* **2002**, *11*, 317.
- Haider, N.; Karlsson, S. *Polym. Degrad. Stab.* **1999**, *64*, 321.
- Bauer, I.; Habicher, W. D.; Korner, S.; Al-Malaika, S. *Polym. Degrad. Stab.* **1997**, *55*, 217.
- Basfar, A. A.; Idriss Ali, K. M.; Mofti, S. M. *Polym. Degrad. Stab.* **2003**, *82*, 229.
- Jia, H.; Wang, H.; Chen, W. *Radiat. Phys. Chem.* **2007**, *76*, 1179.
- Shi, W.; Zhang, J.; Shi, X.-M.; Jiang, G.-D. *Polym. Eng. Sci.* **2007**, *47*, 1480.
- Xiang, X.; Chen, S.; Zhang, J.; Chai, R. *Polym. Eng. Sci.* **2011**, *51*, 624.

34. Xiang, X.; Chen, S.; Zhang, J.; Huang, X. *Polym. Eng. Sci.* **2010**, *50*, 1095.
35. Xiang, X.; Chen, S.; Zhang, J.; Chai, R. *J. Vinyl Addit. Technol.* **2010**, *16*, 23.
36. Xiang, X.; Chai, R.; Chen, S.; Zhang, J. *J. Vinyl Addit. Technol.* **2010**, *16*, 175.
37. Fabiyi, J. S.; McDonald, A. G.; Wolcott, M. P.; Griffiths, P. R. *Polym. Degrad. Stab.* **2008**, *93*, 1405.
38. Ke, Q. Q.; Huang, X. Y.; Wei, P.; Wang, G. L.; Jiang, P. K. *J. Appl. Polym. Sci.* **2007**, *104*, 1920.
39. Sirisinha, K.; Meksawat, D. *Polym. Int.* **2005**, *54*, 1014.
40. Brandrup, J.; Immergut, E. H.; Grulke, E. A. *Polymer Handbook*; Wiley: New York, **1999**.
41. Real, L. P.; Gardette, J.-L. *Polym. Test.* **2001**, *20*, 779.
42. Czanderna, A. W.; Pern, F. J. *Sol. Energ. Mater. Sol. C* **1996**, *43*, 101.
43. Arnaud, R.; Moisan, J. Y.; Lemaire, J. *Macromolecules* **1984**, *17*, 332.
44. Morlat-Therias, S.; Fanton, E.; Gardette, J. L.; Peeterbroeck, S.; Alexandre, M.; Dubois, P. *Polym. Degrad. Stab.* **2007**, *92*, 1873.
45. Pospíšil, J.; Nešpurek, S. *Prog. Polym. Sci.* **2000**, *25*, 1261.
46. Im, S.-H.; Choi, S.-S. *Rapid. Commun. Mass Spectrom.* **2010**, *24*, 2753.
47. Kruczala, K.; Schlick, S. *Macromolecules* **2010**, *44*, 325.
48. Shi, X. M.; Zhang, J.; Li, D. R.; Chen, S. J. *J. Appl. Polym. Sci.* **2009**, *112*, 2358.
49. Chanunpanich, N.; Ulman, A.; Strzhemechny, Y. M.; Schwarz, S. A.; Janke, A.; Braun, H. G.; Kraztmuller, T. *Langmuir* **1999**, *15*, 2089.
50. Boukezzi, L.; Boubakeur, A.; Laurent, C.; Lallouani, M. *Iran Polym. J.* **2008**, *17*, 611.
51. Maria, R.; Rode, K.; Brüll, R.; Dorbath, F.; Baudrit, B.; Bastian, M.; Brendlé, E. *Polym. Degrad. Stab.* **2011**, *96*, 1901.
52. Gugumus, F. *Polym. Degrad. Stab.* **1990**, *27*, 19.
53. Wu, Q.; Qu, B.; Xu, Y.; Wu, Q. *Polym. Degrad. Stab.* **2000**, *68*, 97.
54. Fernando, S. S.; Christensen, P. A.; Egerton, T. A.; White, J. R. *Polym. Degrad. Stab.* **2007**, *92*, 2163.
55. Gugumus, F. *Polym. Degrad. Stab.* **2000**, *67*, 35.
56. Gugumus, F. *Polym. Degrad. Stab.* **2002**, *76*, 95.
57. Abou Zeid, H. M.; Ali, Z. I.; Abdel Maksoud, T. M.; Khafagy, R. M. *J. Appl. Polym. Sci.* **2000**, *75*, 179.
58. Mathot, V. B. F.; Scherrenberg, R. L.; Pijpers, M. F. J.; Bras, W. *J. Therm. Anal. Calorim.* **1996**, *46*, 681.
59. Vanden Eynde, S.; Mathot, V.; Koch, M. H. J.; Reynaers, H. *Polymer* **2000**, *41*, 3437.
60. Liu, Z.; Jin, J.; Chen, S.; Zhang, J. *Polym. Degrad. Stab.* **2011**, *96*, 43.